The orbicular granodiorite of Recoba Hill in the North Patagonian Batholith

*Aníbal Soto¹, Francisco Hervé^{2,3}, Mauricio Calderón⁴, Gianfranco Gregorina³

- ¹ HAEDES, Kortewagenstraat 53B, 9230 Wetteren, Belgium. anibal.soto@haedes.eu
- ² Departamento de Geología, Facultad de Ciencias Físicas y Matemáticas, Universidad de Chile, Plaza Ercilla 803, Santiago, Chile. fherve@ing.uchile.cl
- ³ Carrera de Geología, Facultad de Ingeniería, Universidad Andrés Bello, Av. República 220, Santiago, Chile. fherve@unab.cl, g.gregorina96@gmail.com
- ⁴ Carrera de Geología, Facultad de Ingeniería, Universidad del Desarrollo, Av. Plaza 680, Las Condes, Santiago, Chile. mauriciocalderon@udd.cl
- * Corresponding author: anibal.soto@haedes.eu

ABSTRACT. A small body of orbicular granodiorite crops out on the Recoba Hill, immediately east of the town of Chaitén, in the mainland area called Chiloé continental, in southern Chile. The rock comprises cm-sized igneous cores with a single shell of fine-grained plagioclase-quartz-K-feldspar assemblages. It is hosted in a Miocene granodiorite, and it is crosscut by aplite and mafic dikes. No other mention of orbicular rocks has to date been reported for the >1,000 km long North Patagonian Batholith, suggesting that the conditions necessary for their formation were infrequent. Thermobarometric determinations indicate pressures lower than 2 kbar (less than 6 km depth) for its formation, a level much shallower than the estimated source depth of the older rocks of the batholith.

Keywords: Orbicular rocks, Miocene intrusives, Patagonian Batholith, Hornblende geothermobarometry, Chaitén.

RESUMEN. La granodiorita orbicular del cerro Recoba, Batolito Patagónico Norte, Chaitén. Un pequeño cuerpo de granodiorita orbicular aflora en el cerro Recoba, inmediatamente al este del pueblo de Chaitén, en Chiloé continental, sur de Chile. La roca está compuesta de núcleos ígneos centimétricos cubiertos por un único anillo periférico conformado por agregados de grano fino de cuarzo, plagioclasa y feldespato potásico. Está emplazada en una granodiorita miocena y se presenta cortada por diques aplíticos y máficos. A la fecha, no se han reportado otros afloramientos de rocas orbiculares a lo largo de los más de 1.000 km que constituyen el Batolito Patagónico, lo cual sugiere que las condiciones necesarias para su formación fueron infrecuentes. Determinaciones termobarométricas indican presiones inferiores a 2 kbar (menos de 6 km de profundidad) para su formación, un nivel más somero que el de la mayoría de los estimados para las rocas más antiguas del batolito.

Palabras clave: Rocas orbiculares, Intrusivos miocenos, Batolito Patagónico, Geotermobarometría de hornblenda, Chaitén.

1. Introduction

Orbicular granitoids are a peculiar group of igneous rocks characterized by orbicular texture, in which concentric envelopes of mafic and/or felsic minerals crystallize radially and/or tangentially around central cores of different kind (e.g., Leveson, 1966). Although very unusual, outcrops of these rocks have been observed all around the planet with Finland being the region with more occurrences described (e.g., Lahti, 2005). These orbicular rocks typically occur as a localized phenomenon, of limited extent, in or near the margins of large plutonic bodies (Cox, 1973; Moore and Lockwood, 1973; Lahti, 2005). Even though occurrences of hectometric dimensions have been documented (Godoy, 1997), most outcrops are smaller than 5 meters wide by 30 meters long (e.g., Lahti, 2005). The orbicules tend to be spheroidal to ellipsoidal in shape (Grosse et al., 2010), and their size varies from a few to tens of centimeters, which usually increases as the SiO, content does (Lahti, 2005). In fact, the average diameter of orbicules in ultrabasic rocks is usually less than 5 cm, 5-10 cm in basic rocks, 5-15 cm in intermediate rocks, and 10-25 cm (or even around 40 cm) in granitic rocks (Lahti, 2005). The orbicules can be found clustered, in contact with each other, or as discrete bodies within the matrix. The cores can be hornfels (Sylvester, 2011), schists (Cox, 1973), microgranular mafic enclaves (Sylvester, 2011), megacrystals of potassium feldspar and orthopyroxene (Ort, 1992; Decitre et al., 2002), fragments of comb layering (Moore and Lockwood, 1973; Godoy, 1997) or even fragments of previous orbicules (Smillie and Turnbull, 2014). Regarding the shells, their number can fluctuate between 1 and >40 (e.g., Leveson, 1966), and are typically formed by feldspar, biotite, and/or amphibole, with occasional quartz, pyroxene, tourmaline, and cordierite. The crystals are usually elongated and radially and/or tangentially oriented although massive and granular textures have also been reported (e.g., Leveson, 1966; Niemeyer, 2018). While the composition of the plagioclase in the shells is consistent among neighboring orbicules, the plagioclase in the internal layers is usually more calcic than in the outer layers (Vernon, 1985). The host rocks are almost always igneous, although their composition may vary. Thus, orbicules have been found in granitic, mafic, ultramafic, and carbonatite rocks. The most common host rocks, however, are granites, diorites, and gabbros (e.g., Durant, 2001).

Several theories have been proposed to explain the origin of these rocks. One of the very first was given by Hatch (1888), who suggested the orbicules were formed by zonal and radial crystallization around a core during the solidification stage of a stationary magma. Some years later, Wiik (1899) suggested that orbicules formed when nuclei passed through magmas of various compositions, the same hypothesis that would be used by Sederholm (1928) to explain the origin of the rapakivi texture. Eskola (1938) proposed a migmatitic origin of the matrix and stated that many of the characteristics of these rocks violated the laws of magmatic crystallization, attributing their formation to a metasomatic replacement of pre-existing minerals by hydrothermal fluids instead. Simonen (1950), in agreement with Eskola, suggested that foreign material provided the nuclei for crystallization triggered by an approach to the migmatitic front. Likewise, Leveson (1963) proposed that orbicules formed as an abnormal product of granitization, through diffusion processes that resulted in periodic and discontinuous precipitation or crystallization. The presence of hydrated mineral phases in the orbicules led many authors to invoke the importance of water in their formation. For example, the coexistence of orbicules and comb layering in many outcrops, along with the strong similarity in their textures, motivated Moore and Lockwood (1973) to conclude that there must be a genetic relationship between them. Orbicular rocks would then result from the precipitation of comb layering layers onto rock fragments from water-rich fluids. Elliston (1984), suggested that the magma in which the orbicules formed needed to have the diffusive and rheological properties of a paste or gel made of hydrosilicates. Vernon (1985) argued that structures such as comb layering and orbicular texture would require the absence of nuclei in the magma, which would allow reaching a degree of undercooling such that crystallization is only possible onto solid objects. Since the overheating of magma is a good mechanism for the destruction of nuclei, as demonstrated by experimental results (Lofgren, 1983), Vernon (1985) suggested that overheating could be a common and important factor in conditioning the magma towards the production of most orbicular rocks. These latter ideas gained popularity and have been invoked by many authors to explain the origin of orbicular rocks (e.g., Ort, 1992; Lindh and Näsström, 2006; Grosse et al., 2010; Sylvester, 2011; Smillie and Turnbull, 2014; Díaz-Alvarado et al., 2017).

In northern Chile, several outcrops of orbicular rocks have been described (Fig. 1A). The first one was in the Jurassic Caldera tonalite (Aguirre *et al.*, 1976; Díaz-Alvarado *et al.*, 2017) which is a frequently visited protected National Monument and a geosite of high geological relevance (Sernageomin, 2023). Godoy (1997) near Chañaral and Niemeyer (2018) at Cerros de Lila also recorded orbicular granitoids (Fig. 1A). Further occurrences of similar rocks have been discovered recently in surrounding areas (A. Quilamán, personal communication, 2022).

In southern Chile, at Recoba Hill (42°55'18" S-72°40'35" W), close to the town of Chaitén (Fig. 1B, C), the first author (AS) discovered an outcrop of orbicular rock in a bare rock surface resulting from a landslide that occurred in the 2015-2016 season. Due to the proximity of the outcrop to the city of Chaitén and the importance for the community he referred to it as Chaitenita (Soto, 2019). No previous mentions of orbicular granitoids exist for southern Chile (Pankhurst *et al.*, 1999; Hervé *et al.*, 2007).

The outcrop conditions for this peculiar rock type are described in this work, together with microscope observations of mineral and rock textures, as well as microprobe analysis of the main minerals present. Some preliminary aspects of its genesis are presented as well.

2. Geological context

The Andean range in the surroundings of Chaitén (Fig. 1B) is mainly composed of plutonic rocks that are part of the North Patagonian Batholith (NPB), a plutonic complex of calk-alkaline signature that extends for ~800 kms between latitudes ~40° S and ~47° S (e.g., Pankhurst et al., 1999; Adriasola et al., 2006). The NPB around Chaitén consists of diorite, tonalite, granodiorite, and monzogranite rocks of Jurassic, Cretaceous, and Miocene ages (Sernageomin-BRGM, 1995) which intrude metasandstones, slates, pelitic schists, mafic schists, amphibolites, and gneisses of Devonian-Carboniferous age (Sernageomin-BRGM, 1995). Localized outcrops of Devonian intrusives and their metamorphic envelopes are also present in the area (Hervé et al., 2016). Zircon U-Pb ages from granitoids collected close to the Recoba Hill yielded an age of 15±1 Ma (Sernageomin-BRGM, 1995), giving the Recoba Hill a Miocene age. Neogene to Holocene volcanic and volcaniclastic rocks are also present, including the products of the 2008 eruption of Chaitén volcano

(Major and Lara, 2013) and the first rhyolite eruption to have at least some of its aspects monitored. The eruption consisted of an approximately 2-week-long explosive phase that generated as much as 1 km³ bulk volume tephra (~0.3 km³ dense rock equivalent, which heavily damaged Chaitén (Fig. 1C). Miocene volcanic rocks, in particular, include basaltic to andesitic lavas, dacitic to rhyolitic pyroclastic flows, and dacitic domes (Sernageomin-BRGM, 1995). A ~500 m-wide milonitic zone, associated with a high-angle reverse fault, is observed just 300 meters away from the orbicular rock outcrop (Fig. 1B, C). This shear zone would be part of the Liquiñe-Ofqui fault system, a long and prominent ~N-S structural feature in southern Chile, well-known for serving as a conduit for hydrothermal fluid flow and magma migration (e.g., Cembrano et al., 1996; Pérez-Flores et al., 2016).

3. Methodology

Photographs of the outcrop were taken and subsequently analyzed using the software ImageJ to obtain descriptive statistics of the orbicules, including core size, envelope thickness, axial ratios, area, and morphology. Thin sections of the orbicules, as well as of the felsic and mafic dikes, were studied by using an Olympus CX31-P polarized light microscope at the Department of Geology, University of Chile. The modal compositions were plotted on a QAP diagram through the GeoChemical Data ToolKIT (GCDkit) module for R.

Chemical compositions of minerals were obtained on selected rock samples from the orbicular rock using a CAMECA SX100 EPMA with 5 wavelengthdispersive spectrometers at the Institut für Mineralogie und Kristallchemie, Universität Stuttgart, Germany, under the guidance of Dr. Thomas Theye. Operating conditions were an acceleration voltage of 15 kV, a beam current of 15 nA, a beam size of 7-10 μm (or a focussed beam for very small crystals), and 20 seconds counting time on the peak and on the background of each element. The standards used were natural wollastonite (Si, Ca), natural orthoclase (K), natural albite (Na), natural rhodonite (Mn), synthetic Cr₂O₃ (Cr), synthetic TiO₂ (Ti), natural hematite (Fe), natural baryte (Ba), synthetic MgO (Mg), synthetic Al₂O₂ (Al) and synthetic NiO (Ni). The PaP correction procedure provided by Cameca was applied. Analytical errors of the applied method were reported by Massonne (2012).

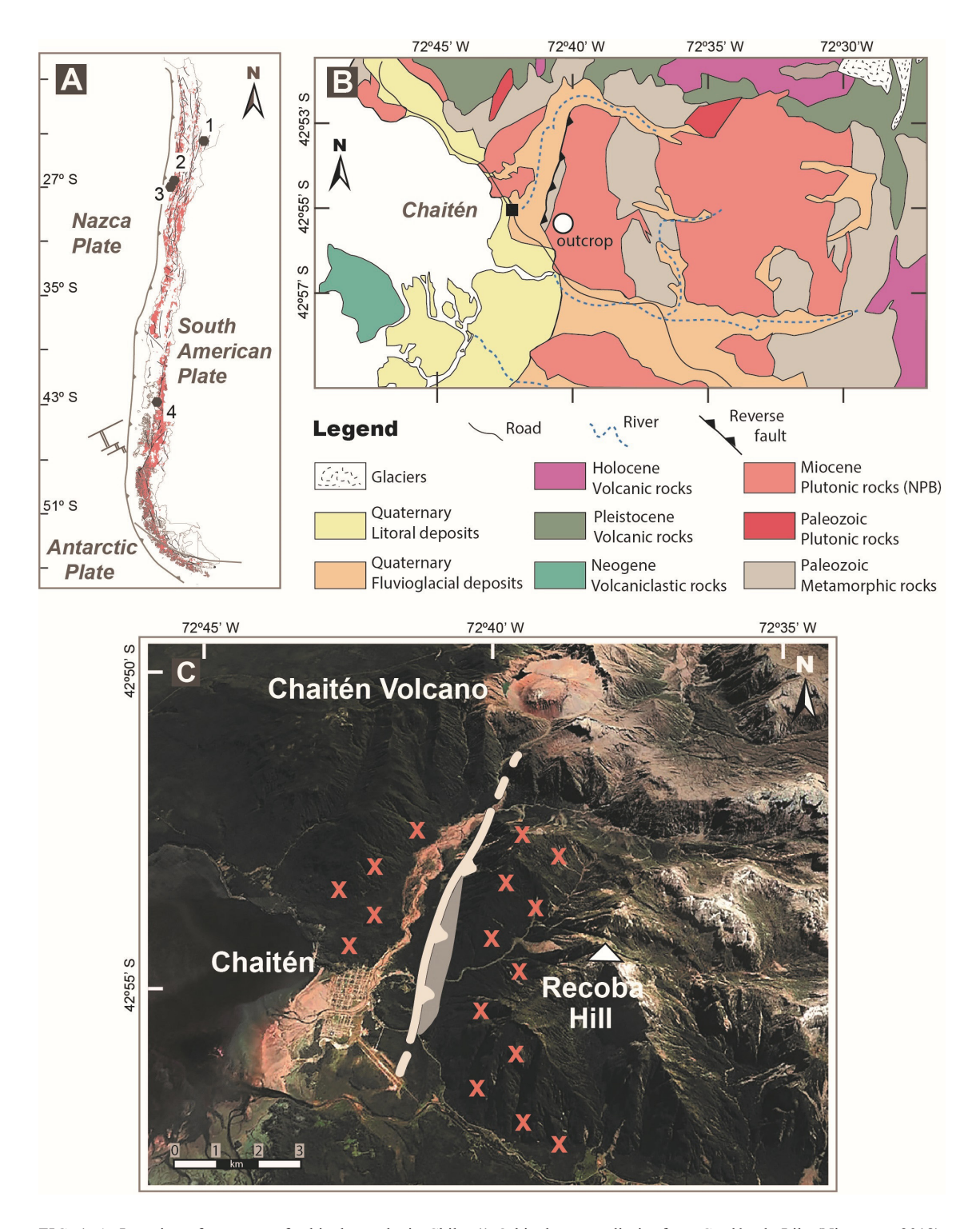


FIG. 1. A. Location of outcrops of orbicular rocks in Chile. 1) Orbicular granodiorite from Cordón de Lila (Niemeyer, 2018).
2) Orbicular gabbro from Quebradas Viejas (Godoy, 1997). 3) Orbicular tonalite from Caldera (Aguirre *et al.*, 1976). 4) This work. B. Geologic map of the Chaitén area extracted from Sernageomin-BRGM (1995). C. Satellite image from Google Earth indicating the main geological features of the area surrounding the orbicular outcrop.

3.1. Field observations

The outcrop is \sim 7x13 m, with an elongated shape and lobulated margins (Fig. 2A). The orbicular domain has an irregular contact with the host rock. The orbicules range in size from 3 to 15 cm along their major axes and have a single leucocratic shell ~3 mm thick on average, developed over subrounded, subspherical gabbroic to dioritic cores (Fig. 2C). In terms of their spatial distribution, the orbicules can appear isolated, tangent to one another, or be completely pressed against each other. Also, some cores show strong alignment near the body margins. The orbicular body is cut by slightly irregular felsic (aplitic) dikes and by a mafic dike (Fig. 2B). The felsic dikes are 10-50 cm-thick and oriented roughly NS, while the mafic dike is 50-70 cm-thick and oriented ~NW-SE. The mafic dike also exhibits foliation along its strike. Some of the orbicules are elongated (Fig. 2C, D), with their longer axes oriented in the ~N-S direction.

The inter-orbicular matrix is lighter colored than the cores, has a phaneritic texture that resembles the granodiorite host rock (Fig. 2C), and it shows a marked ~N-S magmatic foliation at some locations. This matrix does not show a sharp contact with the enclosing rock (Fig. 2D), signaling a physical continuity between the matrix of the orbicular body and the enclosing granodiorite. In the latter, mafic enclaves without shells are also present (Fig. 2E).

Some of the cores exhibit a complete absence of the characteristic leucocratic shell, while others display an incomplete shell of irregular thickness (Fig. 3). Notably, a single mafic core surrounded by a melanocratic shell was also observed (Fig. 3A, B). Some shell fragments can be found dispersed in the inter-orbicular matrix (Fig. 3C).

3.2. Microscopic observations

Mineral compositions of the main constituents of the orbicular rock are shown in a QAP diagram (Fig. 4; Streckeisen, 1976) by using the estimated modes. The orbicule cores vary in lithology from gabbro to quartz gabbro/diorite into monzonite and tonalite. The inter-orbicular matrix is near the boundary between granodiorite and quartz-monzodiorite. The host rock is plotted in the granodiorite field and the felsic dikes consist of leucomonzogranites. The orbicule shells are leucoquartz diorites/gabbro.

Cores

The cores of the orbicules consist of inequigranular, fine- (<1 mm) to medium-grained (1-5 mm), hypidiomorphic rocks (Fig. 5A). In general, the most abundant minerals are plagioclase, quartz and hornblende, with K-feldspar, biotite, titanite, and magnetite as minor phases (Fig. 5B). Plagioclase crystals are strongly altered to saussurite, a mixture of epidote, sericite, zoisite, and chlorite. Albite haloes are common in altered plagioclase crystals included in K-feldspar crystals up to 5 mm long. Some of the cores show acicular apatite with axial ratios of up to 15. Zoned amphibole crystals have a hornblende core and a corona consisting of a complex submicroscopic mineral aggregate. Amphibole also appears as symplectitic intergrowths, some replaced by biotite, with opaque phases. A faint relic ophitic texture is recognized in some cores.

Shells

The shells are almost exclusively composed of saussuritized plagioclase, minor quartz and K-feldspar (Fig. 5C), and traces of amphibole, biotite, epidote, titanite, chlorite, and opaques. Plagioclase forms anhedral to subhedral crystals elongated perpendicular to the contact with the core. These crystals usually stretch along the whole width of the shell. Some have a skeletal or dendritic habit with albite(?) inclusion-free haloes.

Matrix

The matrix represents ~40% of the orbicular rock and is very heterogeneous both in crystal size and in mineral content (Fig. 5D). Pegmatitic domains (>5 mm) grade to a medium-grained, phaneritic granodiorite. The foliation is defined by preferentially oriented plagioclase crystals. Some subrounded plagioclase crystals with albite haloes are included in K-feldspar crystals, similar to those observed in the cores. The matrix also has isolated grains of magnetite, some present as symplectites within amphiboles.

Host rock

The host rock is a hornblende-biotite granodiorite, with predominant saussuritized, weakly oriented prismatic to equant plagioclase crystals. The K-feldspar is slightly altered to fine-grained white mica. Amphibole is present as subhedral prismatic crystals, and is partly replaced by green biotite, which in turn is also dispersed in the rock. Isolated

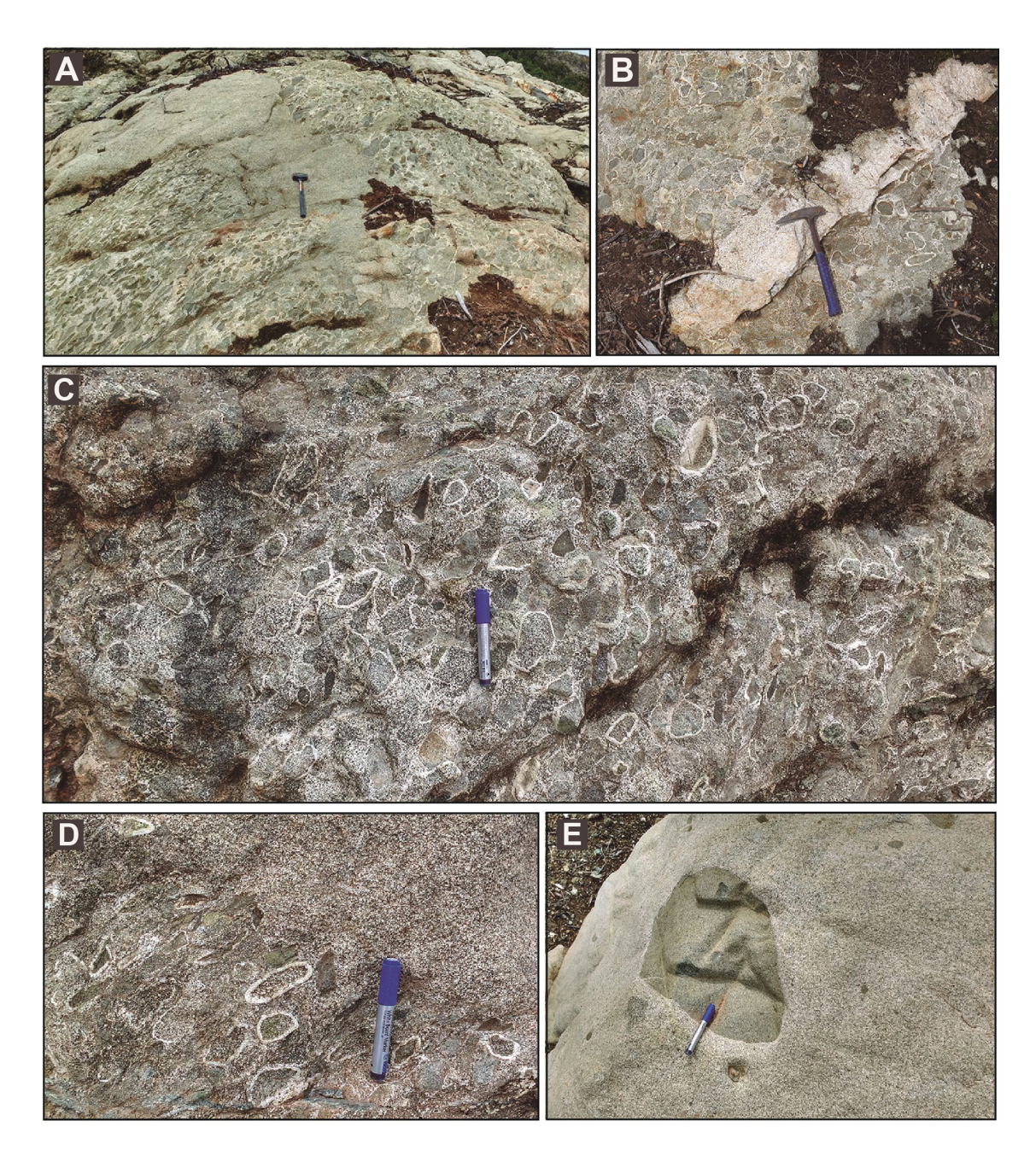


FIG. 2. Diverse field aspects of the orbicular outcrop. A. Field view of the orbicular rock outcrop. Irregular contact with the enclosing granodiorite is shown towards the upper left corner. B. Aplitic dike crosscutting the orbicular body. C. Diversity of core lithologies, some with subangular shapes. D. 5 to 15 cm-long orbicules, some with a noticeable single leucocratic shell developed over subrounded diorite cores. Some of the cores are elongated, with faintly oriented longer axes. The contact between the inter-orbicular matrix and the granodiorite host rock shows an apparent continuity. E. Mafic enclaves in the granodiorite host rock without evident shell development.

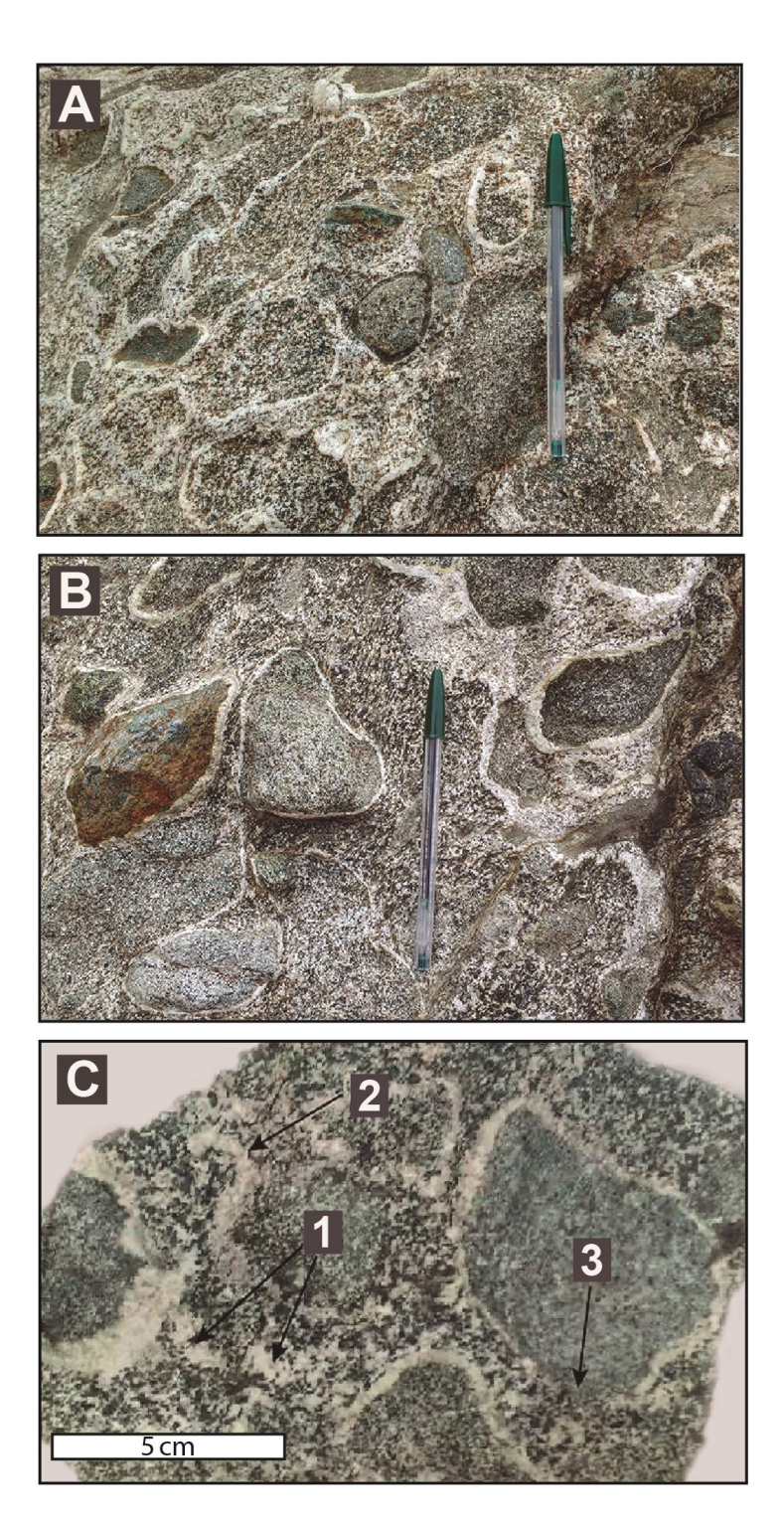


FIG. 3. A. Anomalous orbicule with a dark mineral shell (center) and others lacking the light-colored rim. **B.** Orbicules with rounded shapes immersed in a foliated matrix defined by elongated laths of plagioclase. C. Close-up showing detached fragments of light-colored shells floating in the inter-orbicular matrix (1 and 2), and one orbicule with a partially removed(?) rim (3). Pen is 15 cm long for scale.

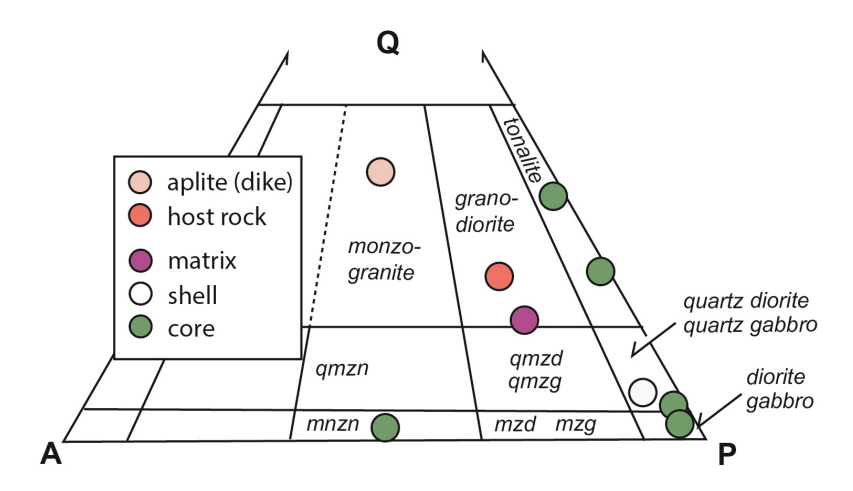


FIG. 4. QAP diagram (after Streckeisen, 1976) of the main constituents of the orbicular rock mentioned in text. Estimated modes.

cubic opaque minerals, euhedral apatite, and titanite are also present.

Aplitic dikes are leucomonzogranites with plagioclase in similar proportion to K-feldspar and quartz. Biotite and hornblende together are less than 5%. Titanite and apatite are accessory minerals.

The mafic dike is a fine-grained foliated microtonalite, with green and strongly oriented biotites and amphiboles, the latter usually perpendicular to the foliation. Saussuritized plagioclase is also present, and titanite, apatite, and isolated opaques are accessory minerals.

4. Mineral chemistry and petrological constraints

The minerals in the core and shell from a ~7 cm-wide orbicule (Fig. 5A) were analyzed with the electron microprobe to constrain crystallization conditions. The chemical compositions of feldspar, amphibole, biotite, titanite, epidote, chlorite, and white mica are shown in table 1. In addition, a classification diagram for amphiboles after Hawthorne *et al.* (2012) is shown in figure 6.

Magnesio-hornblende is the dominant amphibole in unaltered crystal domains, locally altered to actinolite (Fig. 6A, B). In the core, plagioclase is partially altered showing patchy textures, varying from andesine (An₄₂) to oligoclase (An₁₅) (Fig. 6C). K-feldspar is almost a pure phase (Or₉₀) with 10% Na. Biotite shows a molar fraction of iron (X_{Fe}) of 0.4 and is partially altered to chlorite. Epidote is clinozoisite in composition (Ps of 0.2-0.3) and spatially related to albite in the shell of the orbicule.

The cores are characterized by the coexistence of plagioclase, quartz, K-feldspar, amphibole, biotite, titanite, apatite, and magnetite.

Petrological calculations were carried out by using the WinAmptb software of Yavuz and Doner (2017), which estimates the structural formulae of calcic amphiboles based on the International Mineral Association nomenclature scheme (Hawthorne *et al.*, 2012). The method predicts cation site allocations and calculates stoichiometric H₂O and ferric iron contents based on different normalization procedures. Then, the Al-in-hornblende geobarometer of Putirka (2016) was used after the mineral calibration of Hammarstrom and Zen (1986). Results indicate pressures between 1.4 and 1.7 kbar for the crystallization of the core. Different calibrations based on the Holland and Blundy (1994) geothermometer yielded temperature values ranging between 744 and 777 °C.

7. Discussion

The irregular contact between the orbicular body and the host granodiorite (Fig. 2A), suggests that the emplacement of the orbicular granodiorite took place in a mainly hot and ductile crystal mush of granodiorite composition (Fig. 7). Thus, a synplutonic emplacement of the orbicular body is favored. This body could have intruded near the trace of a ~N-S trending fault zone that would have also channelized the fluid flow derived from solidifying magma batches, as suggested by the inter-orbicular matrix foliation and orbicule alignment in some areas.

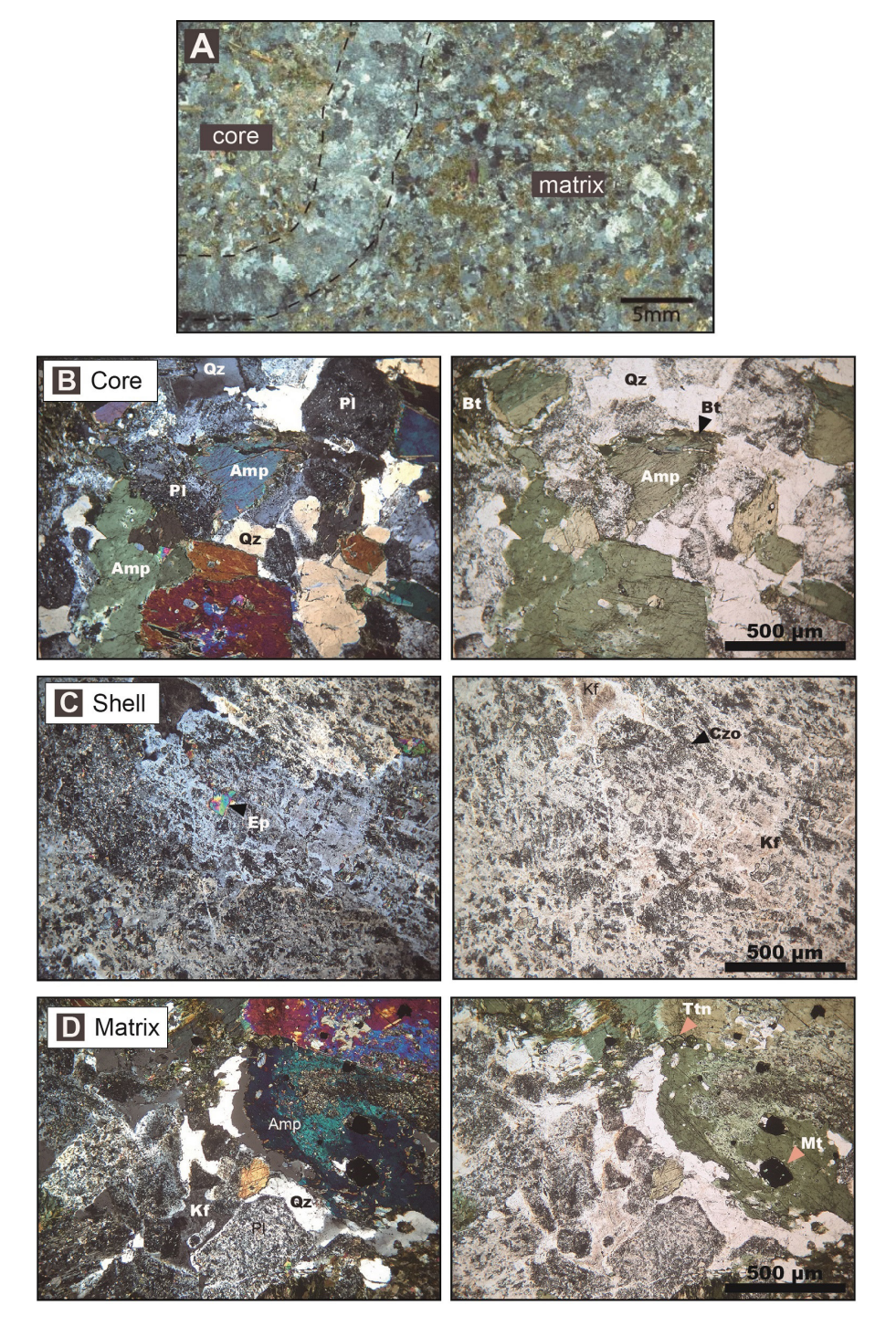


FIG. 5. Images of the orbicular rock analyzed in this study. Photomicrographs under cross-polarized (left panels) and plane-polarized (right panels) light. A. General view showing the core, shell, and matrix components of the orbicular rock. B. Phaneritic texture and mineral composition of the core; one of the analyzed amphibole grains is at the center of the image. C. Radial crystals of saussuritized plagioclase, perpendicular to the contact with the core, along with interstitial quartz in the shell. D. Main mineral constituents of the matrix: amphibole with magnetite inclusions, quartz, partially saussuritized plagioclase, and K-feldspar. A rim of quartz around amphibole can also be noticed. Amp: amphibole; Bt: biotite; Czo: clinozoisite; Ep: epidote; Kf: K-feldspar; Mt: magnetite; Pl: plagioclase; Qz: quartz; Ttn: titanite.

TABLE 1. CHEMICAL COMPOSITION OF MINERALS FROM THE CORE AND SHELL OF THE ORBICULAR GRANODIORITE.

Mineral	Mg-Hbl	Mg-Hbl	Mg-Hbl	Mg-Hbl	Mg-Hbl	Mg-Hbl	Plagioclase	Plagioclase	Plagioclase	Plagioclase	Plagioclase	Plagioclase
Point#	4C	7C	15C	17C	20C	27C	1C	3C	11C	18C	21C	24C
SiO_2	47,8	49,2	46,7	49,9	48,1	48,0	56,9	63,3	62,1	56,5	65,2	60,6
${\rm TiO}_2$	0,9	0,8	1,1	0,1	0,9	1,0	0,0	0,0	0,0	0,0	0,0	0,0
Al_2O_3	6,3	5,8	6,8	5,1	6,3	6,2	26,5	22,0	23,3	25,1	21,6	25,0
FeO	13,4	11,6	14,0	13,8	14,3	12,6	0,1	0,4	0,1	0,9	0,0	0,0
MnO	0,5	0,5	0,5	0,6	0,5	0,5	0,0	0,0	0,0	0,0	0,0	0,0
MgO	14,2	16,0	13,8	14,3	13,6	14,9	0,0	0,1	0,0	0,1	0,0	0,0
CaO	12,1	11,6	11,7	12,4	12,2	11,6	8,8	3,2	4,9	7,1	2,5	6,5
Na_2O	1,0	1,1	1,2	0,7	0,9	1,1	6,7	9,7	9,3	6,2	10,5	8,3
K_2O	0,7	0,6	0,8	0,3	0,6	0,7	0,1	0,4	0,1	2,3	0,1	0,1
Total	96,9	97,1	96,6	97,3	97,3	96,7	99,1	99,2	99,8	98,4	100,0	100,6

Mineral	K-feldspar	Titanite	Titanite	Biotite	Actinolite	Clinozoisite	Clinozoisite	Clinozoisite	Clinozoisite	Clinozoisite	Chlorite	White Mica
Point#	10C	6C	13C	9C	25C	2S	12S	14S	19S	23S	8C	22C
SiO_2	63,6	30,6	30,4	37,6	54,9	37,6	38,1	36,9	36,9	38,1	35,9	46,6
TiO_2	0,0	37,5	37,2	1,3	0,1	0,0	0,0	0,0	0,1	0,0	0,1	0,0
Al_2O_3	18,2	2,2	1,9	15,0	1,4	25,6	24,8	21,3	24,1	26,0	30,2	32,9
FeO	0,1	1,0	1,5	16,5	10,1	9,0	10,2	14,3	10,8	8,4	10,0	2,7
MnO	0,0	0,1	0,0	0,4	0,5	0,2	0,2	0,1	0,2	0,0	0,1	0,0
MgO	0,0	0,0	0,0	14,2	17,6	0,0	0,0	0,0	0,0	0,0	7,6	1,1
CaO	0,0	28,8	29,0	0,1	12,5	23,7	23,3	22,7	23,5	23,7	1,9	0,0
Na_2O	1,1	0,0	0,0	0,1	0,2	0,0	0,0	0,0	0,0	0,0	1,9	0,3
K ₂ O	15,2	0,0	0,0	9,7	0,0	0,0	0,0	0,0	0,0	0,0	0,0	11,2
Total	98,2	100,2	99,9	94,9	97,4	96,1	96,7	95,4	95,6	96,3	87,7	94,9

The letter 'c' next to the point number indicates a mineral from the core, while 's' indicates a mineral from the shell.

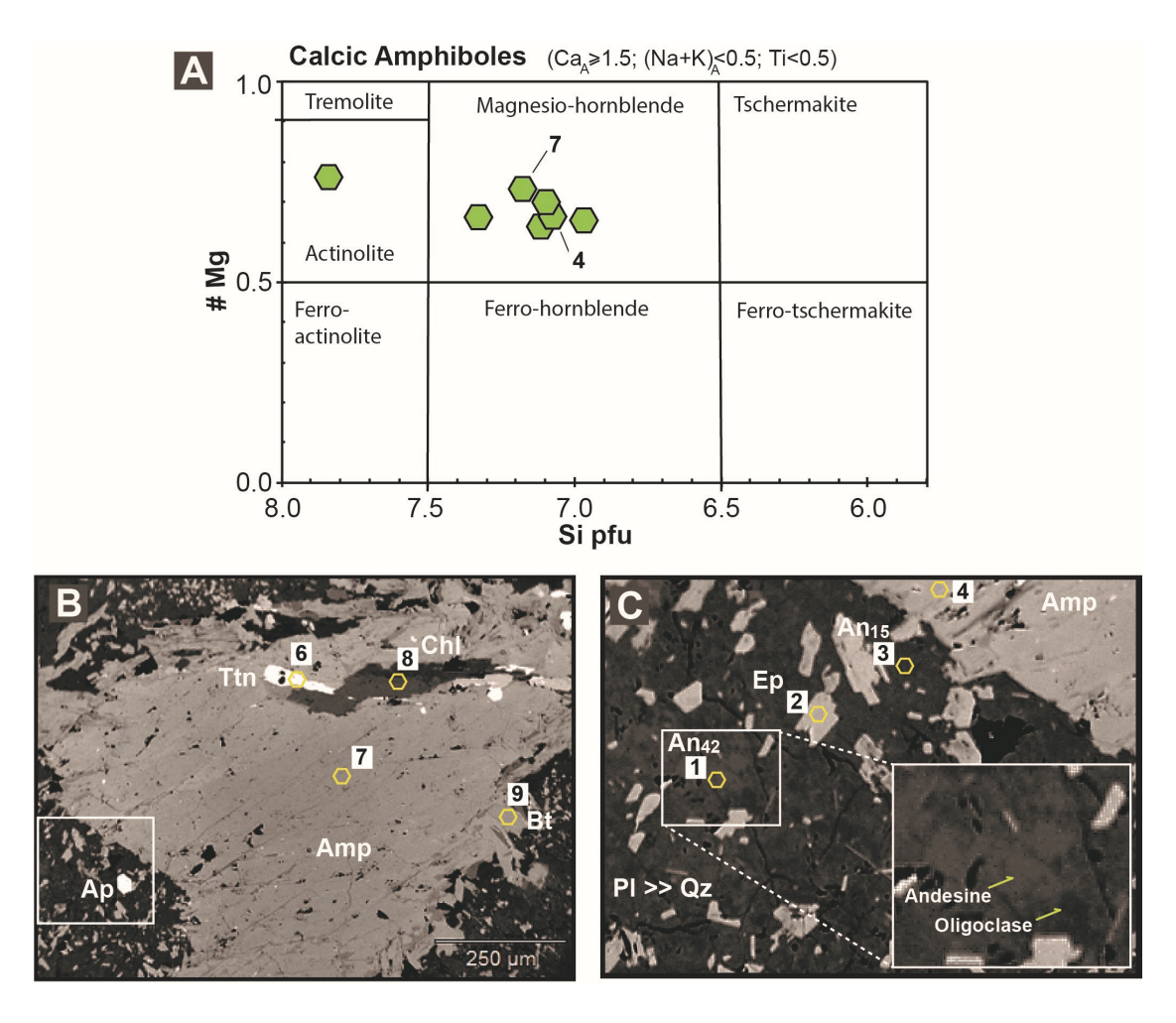


FIG. 6. A. Classification diagram for amphiboles. Magnesio-hornblende cores predominate over thin actinolitic rims. The labeled points 4 and 7 correspond to those used for the calculations of pressure and temperature. Numbers in the back-scattered electron images (B and C) match the EPMA analysis numbers of table 1. Not all amphibole analyses are from the images shown here.

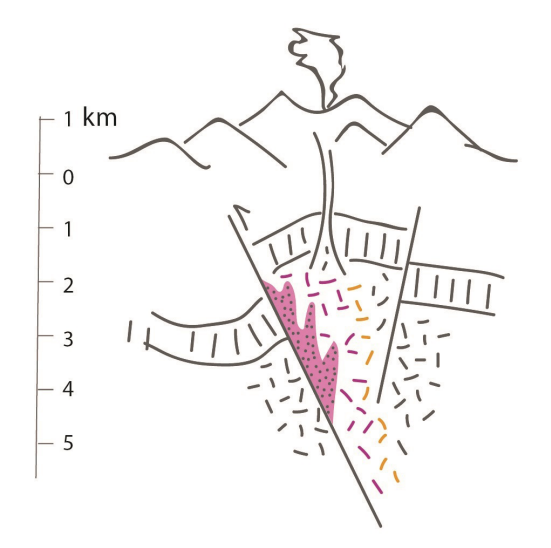
The subrounded morphology of most of the cores, as well as the presence of acicular apatite and of >5 mm-long K-feldspar crystals with plagioclase and titanite inclusions, suggest that at least some of the cores are the result of incomplete mixing and mingling magmatic processes (e.g., Castro et al., 1990; Vernon, 1990; Hibbard, 1991; Baxter and Feely, 2002; Janoušek et al., 2004).

The observation of shell fragments "floating" in the inter-orbicular matrix (Fig. 3C), indicates that the shells also formed in a magmatic, fluidrich environment, which lasted longer than the shells' formation. This is robust evidence to support a magmatic environment against a possible

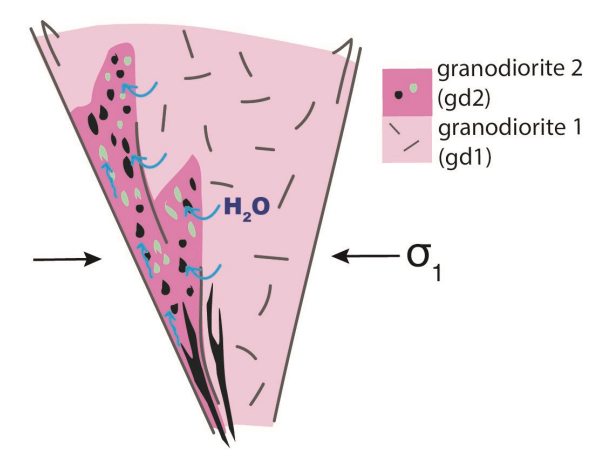
metamorphic one, as indicated by Elliston (1984). This environment could also explain the partial erosion of some shells observed in some orbicules (Fig. 3C). Also, it is possible to establish that the shell formation preceded the compaction of the orbicules, as no shell was observed to envelop two adjoining cores.

Because all shells have uniform thicknesses around the cores, a similar growth rate of the shell in all directions is suggested. As the (010) faces of K-feldspar are perpendicular to the core surface, their growth was probably controlled by a thermal or compositional gradient. The formation of equant to skeletal and dentritic plagioclase crystals suggests

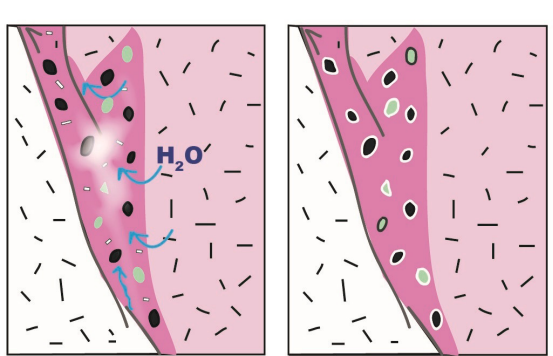
Miocene



Stage 1: granodiorite synplutonic intrusion in a hot and ductile host granodiorite crystal mush.



Zoom stage 1: influx of water within gd2 derived from melts/fluids after crystallization of gd1; mineral disequilibrium, dissolution of solids, precipitation of squeletal plagioclase and K-feldspar in shells (also rare amphibole).



Stage 2: moderate cooling rates, gd2 crystallization, contraction and high-temperature deformation; final crystallization.

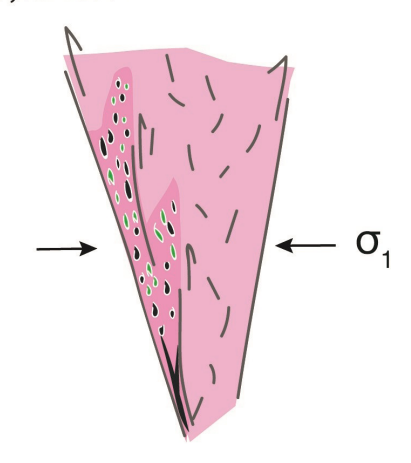


FIG. 7. Sketch of the two-stage petrogenetic model proposed here for the generation of the orbicular body.

a moderate cooling rate (e.g., Lofgren, 1974; Lofgren and Donaldson, 1975), which would ultimately be a consequence of water influx into the magma. When water enters the magma, it reduces the melting point, dissolving small nuclei and delaying nucleation. This causes the magma to become overcooled. When crystallization initiates, rapid cooling results in the formation of dendritic plagioclase texture. Fluid circulation would have been maintained once the magma solidified, producing the observed saussuritization of plagioclase and other replacement features.

The calculated crystallization pressure of the cores (1.4-1.7 kbar) is among the lowest obtained in the North Patagonian Batholith (Hervé *et al.*, 1996). Besides, the calculated temperatures (744-777 °C) are higher than the solidus temperature of diorites (~680 °C) according to recent estimates by Weinberg *et al.* (2023). It is thus proposed that calculated pressure conditions could record the crystallization of magnesio-hornblende from the melt, probably coinciding with a stage of water saturation after the fractional crystallization of plagioclase during

magmatic ascent and cooling. The emplacement of the synplutonic orbicular body occurred at shallow depths (~5-6 km), near the western margin of the host pluton (Fig. 7). Since this pluton is delimited to the west by a fault zone (Fig. 1B, C), this structure probably played a role in its emplacement and later exhumation in late Miocene times.

Summarizing the information above, the following petrogenetic scheme for the origin of the orbicular body is proposed (Fig. 7): 1) a new magma batch ascends, incorporating igneous fragments of different origin during channelized flow through a partially crystallized mush from a previous intrusion. This crystal-poor magma is emplaced at ~5-6 km depth (Fig. 7, stage 1); 2) the new intrusion receives water-rich fluxes from the crystallizing host body, causing magma overheating that digests the small nuclei and delays nucleation processes. Due to this, the magma is subsequently undercooled, causing the mineral shells to rapidly crystallize around the existing igneous cores, creating the orbicules. Before the complete crystallization of the inter-orbicular matrix, the orbicules were affected by compressive and shear forces, resulting in their elongated shapes and mutual ductile contacts (Fig. 7, stage 2).

8. Conclusions

The Recoba Hill Miocene granodiorite pluton includes a small body of orbicular granodiorite. The orbicules consist of cm-sized igneous cores surrounded by single leucocratic fine-grained shells. The evidence presented here favors a synplutonic emplacement of the orbicular body.

The interpretation of diverse textural and mineralogical features indicates that the orbicule-forming process took place in a magmatic environment and not as a solid-state metamorphic reaction. Some crystal habits indicate that the crystallization occurred in moderate undercooling conditions, possibly caused by an influx of water-rich fluids from the host crystallizing rock. The pressures indicated by the Al-in-hornblende geobarometer suggest depths of ~5-6 km in the formation of the orbicular body, much shallower than those estimated elsewhere along the North Patagonian Batholith.

Acknowledgements

This research was made possible by the support of FONDECYT projects 1980547 and 1211906, and the

ANID Exploración project 13220141. Local support by L. Soto, V. Gedda and the community of Chaiten are heartily acknowledged. Expert guidance by Dr. T. Theye allowed the EPMA analysis at Stuttgart University. We are also grateful to Ch. Creixell, J. Díaz-Alvarado, and N. Rodríguez for their invaluable assistance in reviewing this manuscript.

References

- Adriasola, A.C.; Thomson, S.N.; Brix, M.R.; Hervé, F.; Stöckhert, B. 2006. Postmagmatic cooling and late Cenozoic denudation of the North Patagonian Batholith in the Los Lagos region of Chile, 41°-42°15′ S. International Journal of Earth Sciences 95 (3): 504-528. https://doi.org/10.1007/s00531-005-0027-9
- Aguirre, L.L.; Hervé, F.A.; del Campo, M. 1976. An orbicular tonalite from Caldera, Chile. Journal of the Faculty of Science, Hokkaido University. Series 4, Geology and Mineralogy 17 (2): 231-259.
- Baxter, S.; Feely, M. 2002. Magma mixing and mingling textures in granitoids: examples from the Galway Granite, Connemara, Ireland. Mineralogy and Petrology 76 (1): 63-74. https://doi.org/10.1007/s007100200032
- Castro, A.; Moreno-Ventas, I.; de la Rosa, J.D. 1990. Microgranular enclaves as indicators of hybridization processes in granitoid rocks, Hercynian Belt, Spain. Geological Journal 25 (3-4): 391-404. https://doi.org/10.1002/gj.3350250321
- Cembrano, J.; Hervé, F.; Lavenu, A. 1996. The Liquiñe Ofqui fault zone: a long-lived intra-arc fault system in southern Chile. Tectonophysics 259 (1): 55-66. https://doi.org/10.1016/0040-1951(95)00066-6
- Cox, B. 1973. Petrogenesis of orbicular migmatites bordering the Idaho batholith Shoup Idaho. MSc Thesis (Unpublished), University of Montana: 58 p.
- Decitre, S.; Gasquet, D.; Marignac, C. 2002. Genesis of orbicular granitic rocks from the Ploumanac'h Plutonic Complex (Brittany, France): petrographical, mineralogical and geochemical constraints. European Journal of Mineralogy 14 (4): 715-731. https://doi.org/10.1127/0935-1221/2002/0014-0715
- Díaz-Alvarado, J.; Rodríguez, N.; Rodríguez, C.; Fernández, C.; Constanzo, Í. 2017. Petrology and geochemistry of the orbicular granitoid of Caldera, northern Chile. Models and hypotheses on the formation of radial orbicular textures. Lithos 284-285: 327-346. https://doi.org/10.1016/j.lithos.2017.04.017
- Durant, D.G. 2001. Orbicular diorite of Fisher Lake, California: Reverse zoning and oscillatory precipitation mechanisms. Ph.D. Thesis (Unpublished), University of Ottawa: 205 p.

- Elliston, J.N. 1984. Orbicules: An indication of the crystallisation of hydrosilicates, I. Earth-Science Reviews 20 (4): 265-344. https://doi.org/10.1016/0012-8252(84)90021-7
- Eskola, P. 1938. On the esboitic crystallization of orbicular rocks. The Journal of Geology 46 (3): 448-485. https://www.jstor.org/stable/30079612
- Godoy, E. 1997. El gabro orbicular de quebrada Ánimas Viejas, provincia de Chañaral, Chile. *In* Congreso Geológico Chileno, No. 8, Actas 2: 1285-1289. Antofagasta.
- Grosse, P.; Toselli, A.J.; Rossi, J.N. 2010. Petrology and geochemistry of the orbicular granitoid of Sierra de Velasco (NW Argentina) and implications for the origin of orbicular rocks. Geological Magazine 147 (3): 451-468. https://doi.org/10.1017/S0016756809990707
- Hammarstrom, J.M.; Zen, E. 1986. Aluminum in hornblende: An empirical igneous geobarometer. American Mineralogist 71 (11-12): 1297-1313.
- Hatch, F.H. 1888. On the Spheroid-bearing Granite of Mullaghderg, Co. Donegal. Quarterly Journal of the Geological Society 44 (1-4): 548-560. https://doi.org/10.1144/GSL.JGS.1888.044.01-04.37
- Hawthorne, F.C.; Oberti, R.; Harlow, G.E.; Maresch, W.V.; Martin, R.F.; Schumacher, J.C.; Welch, M.D. 2012. Nomenclature of the amphibole supergroup. American Mineralogist 97 (11-12): 2031-2048. https://doi.org/10.2138/am.2012.4276
- Hervé, F.; Pankhurst, R.J.; Demant, A.; Ramírez, E. 1996. Age and Al-in-Hornblende geobarometry in the north patagonian batholith, Aysen, Chile. *In* Third International Symposium on Andean Geodynamics (ISAG): 579-582. Saint Malo.
- Hervé, F.; Pankhurst, R.J.; Fanning, C.M.; Calderón, M.; Yaxley, G.M. 2007. The South Patagonian batholith: 150 my of granite magmatism on a plate margin. Lithos 97 (3-4): 373-394. https://doi.org/10.1016/j. lithos.2007.01.007
- Hervé, F.; Calderon, M.; Fanning, C.M.; Pankhurst,
 R.J.; Fuentes, F.; Rapela, C.W.; Correa, J.; Quezada,
 P.; Marambio, C. 2016. Devonian magmatism in the accretionary complex of southern Chile.
 Journal of the Geological Society 173 (4): 587-602.
 https://doi.org/10.1144/jgs2015-163
- Hibbard, M.J. 1991. Textural anatomy of twelve magma-mixed granitoid systems. *In* Enclaves and granite petrology (Didier, J.; Barbarin, B.; editors). Developments in Petrology 13: 431-444.
- Holland, T.; Blundy, J. 1994. Non-ideal interactions in calcic amphiboles and their bearing on amphibole-

- plagioclase thermometry. Contributions to Mineralogy and Petrology 116 (4): 433-447. https://doi.org/10.1007/BF00310910
- Janoušek, V.; Braithwaite, C.J.R.; Bowes, D.R.; Gerdes, A. 2004. Magma-mixing in the genesis of Hercynian calc-alkaline granitoids: an integrated petrographic and geochemical study of the Sázava intrusion, Central Bohemian Pluton, Czech Republic. Lithos 78 (1): 67-99. https://doi.org/10.1016/j. lithos.2004.04.046
- Lahti, S.I. 2005. Orbicular rocks in Finland, 1st edition. Geological Survey of Finland: 177 p. Espoo, Finland.
- Leveson, D.J. 1963. Orbicular rocks of the Lonesome mountain area, Beartooth Mountains, Montana and Wyoming. Geological Society of America Bulletin 74 (8): 1015-1040. https://doi.org/10.1130/0016-7606(1963)74[1015:OROTLM]2.0.CO;2
- Leveson, D.J. 1966. Orbicular Rocks: A Review. Geological Society of America Bulletin 77 (4): 409-426. https://doi. org/10.1130/0016-7606(1966)77[409:ORAR]2.0.CO;2
- Lindh, A.; Näsström, H. 2006. Crystallization of orbicular rocks exemplified by the Slättemossa occurrence, southeastern Sweden. Geological Magazine 143 (5): 713-722. https://doi.org/10.1017/S001675680600210X
- Lofgren, G. 1974. An experimental study of plagioclase crystal morphology; isothermal crystallization. American Journal of Science 274 (3): 243-273. https://doi.org/10.2475/AJS.274.3.243
- Lofgren, G.E. 1983. Effect of heterogeneous nucleation on basaltic textures: a dynamic crystallization study. Journal of Petrology 24 (3): 229-255. https://doi.org/10.1093/petrology/24.3.229
- Lofgren, G.E.; Donaldson, C.H. 1975. Curved branching crystals and differentiation in comb-layered rocks. Contributions to Mineralogy and Petrology 49 (4): 309-319. https://doi.org/10.1007/BF00376183
- Major, J.J.; Lara, L.E. 2013. Overview of Chaitén Volcano, Chile, and its 2008-2009 eruption. Andean Geology 40 (2): 196-215. https://dx.doi.org/10.5027/andgeoV40n2-a01
- Massonne, H.-J. 2012. Formation of amphibole and clinozoisite-epidote in eclogite owing to fluid infiltration during exhumation in a subduction channel. Journal of Petrology 53 (10): 1969-1998. https://doi.org/10.1093/petrology/egs040
- Moore, J.G.; Lockwood, J.P. 1973. Origin of comb layering and orbicular structure, Sierra Nevada Batholith, California. Geological Society of America Bulletin 84 (1): 1-20. https://doi.org/10.1130/0016-7606(1973)84%3C1:OO CLAO%3E2.0.CO;2

- Niemeyer, H. 2018. The orbicular granodiorite from Cordón de Lila, Antofagasta Region, Chile. Andean Geology 45 (1): 104-109. http://dx.doi.org/10.5027/ andgeoV45n1-3114
- Ort, M.H. 1992. Orbicular volcanic rocks of Cerro Panizos: Their origin and implications for orb formation. Geological Society of America Bulletin 104 (8): 1048-1058. https://doi.org/10.1130/0016-7606(1992)104%3C1 048:OVROCP%3E2.3.CO;2
- Pankhurst, R.J.; Weaver, S.D.; Hervé, F.; Larrondo, P. 1999. Mesozoic-Cenozoic evolution of the North Patagonian Batholith in Aysen, southern Chile. Journal of the Geological Society 156 (4): 673-694. https://doi.org/10.1144/gsjgs.156.4.0673
- Pérez-Flores, P.; Cembrano, J.; Sánchez-Alfaro, P.; Veloso, E.; Arancibia, G.; Roquer, T. 2016. Tectonics, magmatism and paleo-fluid distribution in a strike-slip setting: Insights from the northern termination of the Liquiñe-Ofqui fault System, Chile. Tectonophysics 680: 192-210. https://doi.org/10.1016/j.tecto.2016.05.016
- Putirka, K. 2016. Amphibole thermometers and barometers for igneous systems and some implications for eruption mechanisms of felsic magmas at arc volcanoes. American Mineralogist 101 (4): 841-858. https://doi.org/10.2138/am-2016-5506
- Sederholm, J.J. 1928. On orbicular granites: spotted and nodular granites etc. and on the rapakivi texture. Suomen Geologinen Toimijunta: 105 p. Helsinki.
- Sernageomin. 2023. Geositios de Chile: Una mirada a sus maravillas geológicas. Servicio Nacional de Geología y Minería: 144 p. Santiago.
- Sernageomin-BRGM. 1995. Carta Metalogénica Xª Región sur. Servicio Nacional de Geología y Minería Bureau de Recherches Géologiques et Minières, Informe Registrado IR-95-05 (Inédito), 4 Tomos, 10 Vols., 95 mapas diferentes escalas. Santiago.
- Simonen, A. 1950. Three new boulders of orbicular rock in Finland. Suomen Geologisen Seuran Julkaisuja, 150: 31-38.

- Smillie, R.W.; Turnbull, R.E. 2014. Field and petrographical insight into the formation of orbicular granitoids from the Bonney Pluton, southern Victoria Land, Antarctica. Geological Magazine 151 (3): 534-549. https://doi.org/10.1017/S0016756813000484
- Soto, A. 2019. La granodiorita orbicular del Cerro Recoba, Batolito Patagónico Norte, Chaitén. Memoria para optar al título de Geólogo (Inédito), Universidad de Chile: 58 p.
- Streckeisen, A. 1976. To each plutonic rock its proper name. Earth-Science Reviews 12 (1): 1-33. https://doi.org/10.1016/0012-8252(76)90052-0
- Sylvester, A.G. 2011. The nature and polygenetic origin of orbicular granodiorite in the Lower Castle Creek pluton, northern Sierra Nevada batholith, California. Geosphere 7 (5): 1134-1142. https://doi.org/10.1130/GES00664.1
- Vernon, R.H. 1985. Possible role of superheated magma in the formation of orbicular granitoids. Geology 13 (12): 843-845. https://doi.org/10.1130/0091-7613(1985)13%3C843:PROSMI%3E2.0.CO;2
- Vernon, R.H. 1990. Crystallization and hybridism in microgranitoid enclave magmas: Microstructural evidence. Journal of Geophysical Research, Solid Earth 95 (B11): 17849-17859. https://doi.org/10.1029/ JB095iB11p17849
- Weinberg, R.F.; Moyen, J.-F.; Yi, J.-K.; Zhu, D.-C.; Nebel, O.; Chen, S.; Wang, Q. 2023. Using zircons to disentangle back-veining and hybridization of diorite dykes: an example from the Gangdese arc, Tibet. Journal of Petrology 64 (3): 20 p. https://doi.org/10.1093/petrology/egad010
- Wiik, F.J. 1899. Om de primitiva formationernas geologi med särskild hänsyn till Finlands geologiska förhållanden. Finska Vetenskaps-Societeten: 275 p. Helsingfors.
- Yavuz, F.; Döner, Z. 2017. WinAmptb: A Windows program for calcic amphibole thermobarometry. Periodico di Mineralogia 86 (2): 135-167. https://doi. org/10.2451/2017PM710